INL/CON-19-55454-Revision-0

Uncollided-Flux Treatment for Discrete-Ordinate Radiation Transport Solutions in the Rattlesnake Code System

Logan H Harbour, Jean Ragusa, Yaqi Wang, Sebastian Schunert, Derek R Gaston, Mark D DeHart

August 2019

The INL is a U.S. Department of Energy National Laboratory
operated by Battelle Energy Alliance

INL/CON-19-55454-Revision-0

Uncollided-Flux Treatment for Discrete-Ordinate Radiation Transport Solutions in the Rattlesnake Code System

Logan H Harbour, Jean Ragusa, Yaqi Wang, Sebastian Schunert, Derek R Gaston, Mark D DeHart

August 2019

Idaho National Laboratory
Idaho Falls, Idaho 83415

http://www.inl.gov

Prepared for the
U.S. Department of Energy

Under DOE Idaho Operations Office
Contract DE-AC07-05ID14517

UNCOLLIDED-FLUX TREATMENT FOR DISCRETE-ORDINATE RADIATION TRANSPORT SOLUTIONS IN THE RATTLESNAKE CODE SYSTEM

Logan Harbour[1], Jean Ragusa[1], Yaqi Wang[2], Sebastian Schunert[2]
Derek Gaston[3], and Mark DeHart[2]

[1]Department of Nuclear Engineering
Texas A&M University, College Station, TX, 77845

[2]Reactor Physics & Safety Analysis, [3]Modeling & Simulation
Idaho National Laboratory, Idaho Falls, ID 83415

loganharbour@tamu.edu

ABSTRACT

We present the uncollided-flux treatment implemented in the Rattlesnake code system of the Idaho National Laboratory (INL). The ray-tracing method employed is capable of handling various types of finite-element meshes. Uncollided-flux techniques are necessary to capture streaming in low-density regions, such as the ones found in the TREAT test reactor at INL. Numerical results are presented.

KEYWORDS: uncollided flux; first-collision source; ray effects; ray tracing

1. INTRODUCTION

In many radiation transport problems containing a localized fixed source, the uncollided component of the angular flux (i.e., the flux of particles that transport directly from the source and have yet to undergo a collision) can be highly anisotropic. Angular discretization techniques, be it S_N discrete-ordinates or spherical harmonics, can exhibit large errors (known as "ray effects" for S_N methods) due to the insufficient angular resolution [1]. For example, when the source is localized, with narrow streaming gaps presents, the number of angular degrees of freedom to capture correctly the uncollided flux solution, which is non-zero only in a narrow solid-angle cone, can be prohibitive. Such situations are found, for instance, in the Transient Reactor Test Facility (TREAT) at Idaho National Laboratory (INL). In TREAT transient tests, a small experimental capsule containing the fuel to be tested in subjected to short bursts of intense, high-power neutron radiation. Fission occurs in the experimental fuel and the fast neutrons thus emitted stream several meters away, being collimated by an "hodoscope" system.

Hodoscopes are generally constructed of several segments of filter, collimators and detectors; the combination of these segments is then used to infer where the particle passed through hodoscope by the location at which the particle is detected. A fast-neutron hodoscope is used to detect fast neutrons emitted as a result of fissions in a nuclear fuel sample. The system (illustrated in Figure

1) was developed to provide a imaging system to view fuel motion and failure during rapid power excursions, albeit with a limited degree of spatial resolution. It relies on fast neutrons born in the test sample(s) to travel approximately 3 m through air to reach the detector pairs. It uses collimators and two sets of detectors located outside the reactor core for fast neutron measurements [2]. The slots within the collimator have a surface area of 0.85 cm^2 at the detector interface, which at the 3 m from the test sample is a fractional solid angle of roughly 7×10^{-7} sr.

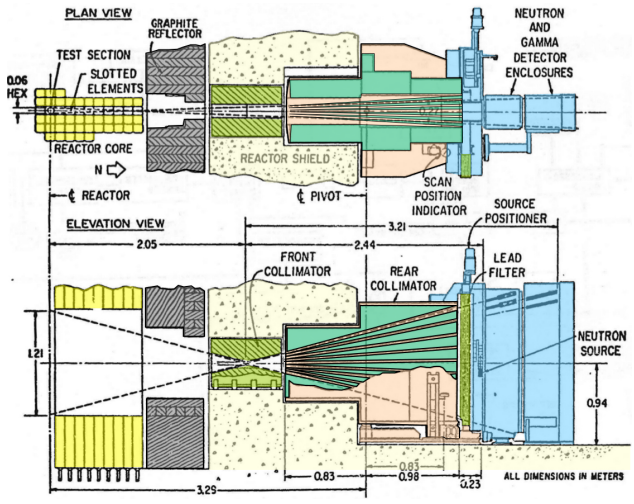

Figure 1: Plan and elevation views of a cross-section of TREAT, showing the relative orientation of the core, a test item, structural materials, and the hodoscope [2].

It has been recognized that an analytical or semi-analytical treatment of the uncollided angular flux, coupled with a discrete ordinate treatment of the collided angular flux, can yield dramatic improvements in accuracy and computational efficiency. This treatment of the uncollided flux is termed the first-collision source treatment and will be the focus of this work.

Many transport codes have implemented uncollided flux algorithms for the purpose of first collision source treatments, such as ATILLA [3], AETIUS [4], PARTISN [5], Denovo [6], GRTUNCL3D [7], and FNSUNCL3 [8]. Several of these examples are implemented only in serial or are only scalable to a few ranks [3,5]. All of the above have the capability to utilize ray-tracing to obtain the uncollided flux, but some only have support for point sources [6]. Volumetric source support is important for the purpose of modeling physically realistic problems. In addition, the scalability of the ray-tracing algorithms are not discussed. When utilizing distributed meshes, there is great concern for the scalability when localized sources are present due to excessive communication. Of the above, all but ATILLA [3] and AETIUS [4] utilize brick-type meshes to represent the problem geometry. This could potentially be a significant drawback to meshing problems with complex shapes and curved surfaces, as are prevalent in nuclear reactor analysis.

In this paper, we present an uncollided-flux treatment for arbitrary finite-element meshes. It is implemented in the Rattlesnake code, based on the MOOSE multiphysics simulation platform. The remainder of the paper is as follows: in Section 2, a review of the uncollided-flux technique is presented, in Section 3, it is specialized for finite-element grids. Results are presented in Section 4

and conclusions in Section 5.

2. BACKGROUND ON THE UNCOLLIDED-FLUX TECHNIQUE

2.1. Generalities

Using operator notation, the transport problem can be viewed as

$$\mathbf{L}\psi = \mathbf{H}\psi + \mathbf{Q}\,, \tag{1}$$

where $\mathbf{L}$ is the streaming and collision operator ($\mathbf{\Omega}\cdot\mathbf{\nabla} + \sigma_t$ and boundary conditions), $\mathbf{H}$ is the scattering operator, $\mathbf{Q}$ is an extraneous source, and ψ is the angular flux solution. In the discrete-ordinate method, an iterative approach is used:

$$\mathbf{L}\psi^{(\ell+1)} = \mathbf{H}\psi^{(\ell)} + \mathbf{Q}\,. \tag{2}$$

With the first guess $\psi^{(0)} = 0$, $\psi^{(1)} = \mathbf{L}^{-1}\mathbf{Q}$ is the angular flux due exclusively to the presence of the external sources ($\mathbf{Q}$ and incident boundary conditions), that is, $\psi^{(1)}$ is the uncollided flux. Then, in the iterative process, $\psi^{(1)}$ is used to compute the first-collision source $\mathbf{H}\psi^{(1)}$ and $\psi^{(2)}$ will represent the flux of neutrons have had at most one collision event.

Using the discrete-ordinate to obtain the uncollided flux in the above process leads to the largest angular errors because S_N method suffers from ray effects with the angular quadratures only being rotationally invariant by octant. By semi-analytically treating the $\mathbf{L}$ operator to obtain the uncollided flux (rather than using S_N transport sweeps), we strive to mitigate the ray effects.

2.2. First-Collision Source Treatment

The $\mathbf{L}$ operator in Eq. (1) can be inverted semi-analytically with great accuracy through ray-tracing in arbitrary geometries. Hence, the idea of decomposing the angular flux into collided (c) and uncollided (u) components as $\psi = \psi^u + \psi^c$. The uncollided component is obtained from

$$\mathbf{L}^{\text{RT}}\psi^u = \mathbf{Q}\,,$$

where the superscript RT denotes ray-tracing. Using the uncollided flux, a first-collided scattering source, $\mathbf{H}\psi^{u,\text{RT}}$, is created for the collided equation and replaces the external source as

$$\mathbf{L}^{\text{SN}}\psi^c = \mathbf{H}\psi^c + \mathbf{H}\psi^u\,,$$

where the superscript SN denotes the S_N solve. Similarly to Eq. (2), a source iteration process is then employed to solve the above equation:

$$\mathbf{L}^{\text{SN}}\psi^{c,(\ell+1)} = \mathbf{H}\psi^{c,(\ell)} + \mathbf{H}\psi^u\,.$$

Upon convergence (superscript ∞), the total angular flux is obtained by summation:

$$\psi = \psi^u + \psi^{c,(\infty)}\,.$$

3. UNCOLLIDED-FLUX TREATMENT IN FINITE-ELEMENT MESHES

The Rattlesnake radiation transport code of INL is based on the MOOSE framework, itself based on the libMesh finite-element library. Thus, in order to implemented the uncollided flux technique in Rattlesnake, it is necessary to adapt the formalism for finite-element grids. For now, we will show the equations only for the uncollided scalar flux by assuming isotropic scattering. The method can be extended to evaluate higher-order angular flux moments without fundamental difficulty. Due to the current limitations of the ray-tracer in MOOSE (see Section 3.3), we currently can only compute cell-averaged uncollided values.

We compute the cell-averaged uncollided flux for any target cells of the mesh, K (where $K \in (\mathcal{D} \backslash \mathcal{S})$) that are different than a single source cell, $K' \in \mathcal{S}$). With this notation, $\mathcal{D}$ describes the entire domain and $\mathcal{S}$ describes the subset of the domain that contains the source(s). The method is presented for one source at a time and the uncollided flux is computed in all cells due to that one source (we distinguish between the target cell containing that source, $K = K'$, or not, $K \neq K'$).

We introduce the following notation for convenience: $\tau(\mathbf{r}_1, \mathbf{r}_2)$ is the optical thickness from $\mathbf{r}_1$ to $\mathbf{r}_2$, $\mathbf{\Omega}(\mathbf{r}_1, \mathbf{r}_2) = (\mathbf{r}_2 - \mathbf{r}_1) / \left\|\mathbf{r}_1 - \mathbf{r}_2\right\|$, $S(\mathbf{r}, \mathbf{\Omega})$ is the volumetric source strength at $\mathbf{r}$ in direction $\mathbf{\Omega}$ (n/cm^3·s·str) and V_K is the volume of cell K (cm^3).

3.1. Target cell $\neq$ source cell ($K \neq K'$)

The exact uncollided scalar flux at $\mathbf{r} \in K$ as a result of a volumetric source cell K' is

$$\phi_K^{K'}(\mathbf{r}) = \int_{K'} \frac{\exp(-\tau(\mathbf{r}', \mathbf{r}))}{\left\|\mathbf{r} - \mathbf{r}'\right\|^2} S(\mathbf{r}', \mathbf{\Omega}(\mathbf{r}', \mathbf{r}))\, d^3 r' \,,$$

Introduce spatial quadrature set $\{\mathbf{r}_q, w_q\}$ in the target cell K where $\sum_q w_q = V_K$ and spatial quadrature set $\{\mathbf{r}_{q'}, w_{q'}\}$ in the source cell K' where $\sum_{q'} w_{q'} = V_{K'}$. Then, integrate numerically over the target cell and divide by its volume to obtain the approximate, cell-averaged uncollided scalar flux in cell K as a result of source cell K':

$$\bar{\phi}_K^{K'} \approx \frac{1}{V_K} \sum_q w_q \sum_{q'} w'_q \frac{\exp(-\tau(\mathbf{r}_{q'}, \mathbf{r}_q))}{\left\|\mathbf{r}_{q'} - \mathbf{r}_q\right\|^2} S(\mathbf{r}_{q'}, \mathbf{\Omega}(\mathbf{r}_{q'}, \mathbf{r}_q)) \,. \tag{3}$$

3.2. Target cell = source cell ($K = K'$)

With Eq. (3), the uncollided flux was computed using Green's function which contains a $1/R^2$ term. Hence, computing the uncollided flux inside the source cell is problematic when a single spatial quadrature is used. To combat this we begin with the exact cell-averaged scalar flux in a given cell K due to the source in K:

$$\bar{\phi}_K^K = \frac{1}{V_K} \int_K d^3 r \int_{K'} d^3 r' \, \frac{\exp(-\tau(\mathbf{r}', \mathbf{r}))}{\left\|\mathbf{r}' - \mathbf{r}\right\|^2} S(\mathbf{r}', \mathbf{\Omega}(\mathbf{r}', \mathbf{r})) \,.$$

We will eliminate the $1/\left\|\mathbf{r}' - \mathbf{r}\right\|^2$ term by introducing the change of variable $\mathbf{r}' = \mathbf{r} - \mathbf{R} = \mathbf{r} - R\mathbf{\Omega}$, $d^3 r' = d^3 r = R^2 dR d\Omega$ to obtain

$$\bar{\phi}_K^K = \frac{1}{V_K} \int_K d^3 r \int_{4\pi} d\Omega \int_0^{R_+(\mathbf{r}, \mathbf{\Omega})} dR \, \exp(-\tau(\mathbf{r} - R\mathbf{\Omega}, \mathbf{r})) S(\mathbf{r} - R\mathbf{\Omega}, \mathbf{\Omega}) \,, \tag{4}$$

where $R_+(\mathbf{r}, \mathbf{\Omega})$ is the distance from $\mathbf{r}$ to the intersection of the trajectory at $\mathbf{r}$ in the direction $\mathbf{\Omega}$ with the surface of K. If material is spatially constant in K, the integral over the trajectory in Eq. (4) (with a removed independent volumetric source term) can be evaluated analytically as

$$\int_0^{R_+(\mathbf{r},\mathbf{\Omega})} dR\ \exp(-\tau(\mathbf{r} - R\mathbf{\Omega}, \mathbf{r})) = \frac{1}{\Sigma_t}\left(1 - e^{-\Sigma_t R_+(\mathbf{r},\mathbf{\Omega})}\right) ,$$

and if the material is not spatially constant in K, we introduce the 1D quadrature set $\{R_q, w_q\}$ with $\sum_q w_q = R_+(\mathbf{r}, \mathbf{\Omega})$ along the ray direction $\mathbf{\Omega}$ as

$$\int_0^{R_+(\mathbf{r},\mathbf{\Omega})} dR\ \exp(-\tau(\mathbf{r} - R\mathbf{\Omega}, \mathbf{r}))S(\mathbf{r} - R\mathbf{\Omega}, \mathbf{\Omega}) \approx \sum_q w_q \exp(-\tau(\mathbf{r} - R_q\mathbf{\Omega}, \mathbf{r}))S(\mathbf{r} - R_q\mathbf{\Omega}, \mathbf{\Omega}) .$$

Lastly, introduce angular quadrature set $\{\mathbf{\Omega}_d, \omega_d\}$, 3D quadrature set $\{\mathbf{r}_j, w_j\}$ with $\sum_j w_j = V_K$ to obtain

$$\bar{\phi}_K^K \approx \frac{1}{V_K}\sum_j w_j \sum_d \omega_d \begin{cases} \sum_q w_q \exp(-\tau(\mathbf{r}_q, \mathbf{r}_j))S(\mathbf{r}_j - R_q\mathbf{\Omega}_d, \mathbf{\Omega}_d) , & \text{non-const. mat.} \\ S(\mathbf{\Omega}_d)\frac{1}{\Sigma_t}\left(1 - \exp(-\Sigma_t R_+(\mathbf{r}_j, \mathbf{\Omega}_d))\right) , & \text{const. mat., } \Sigma_t \neq 0 \\ S(\mathbf{\Omega}_d)R_+(\mathbf{r}_j, \mathbf{\Omega}_d) & \text{const. mat., } \Sigma_t = 0 \end{cases} . \tag{5}$$

3.3. Ray-tracing

The ray-tracing module is currently under development by D. Gaston for the use in MOCkingbird [9], a neutron transport code using the method of characteristics (MOC) written in the MOOSE framework. It provides a straight-forward framework for the tracing of rays in an arbitrary mesh.

Standard ray tracing algorithms utilize a bulk synchronous method of ray generation and propagation, which is to simply generate all of the rays at the beginning of the process and after all are generated propagate and communicate them. The MOOSE ray-tracing module utilizes what it terms the SMART (Scalable Massively Asynchronous Ray Tracing) method, in which rays are generated in *chunks* and are propagated and communicated as deemed necessary by the algorithm. An optimal ray chunk size and propagation threshold have been set such that a processor will typically generate more rays only if it does not have a sufficient number of rays buffered to be propagated and communicated.

It is important to note that the ray-tracing MOOSE module currently supports storing only constant values on each element for the time being, which limits the uncollided scalar flux solution to cell-averaged values. Therefore, a temporary workaround is required to enable a higher-fidelity ray-tracing solution for the purpose of the uncollided flux treatment in Rattlesnake. The mesh that is used to compute the uncollided flux is refined once-more than the mesh that is used to compute the discrete-ordinates solution. The more refined, cell-averaged uncollided flux is then projected onto the once less refined discrete-ordinates mesh using first-order L2 Lagrange variable in MOOSE. Said variable is a linear discontinuous representation with one degree of freedom per element node and eight nodal values per hexahedral element. This method is currently very costly due to the

increased number of rays and ray segments required, which has significant impacts on parallel performance. However, it makes possible verification of the implementation thus far.

3.4. Implementation

The general process followed to trace the rays in a distributed mesh is as follows:

1. Each processor stores the local ray "targets" (portions of the domain where the uncollided flux is desired). This is a list of elements and the points in each element that need to be traced to, in addition to the necessary weights if quadrature is used.
2. The list of local ray targets is serialized and communicated to all other processors so that each source processor has the knowledge of the end points of each ray that it spawns.
3. Each processor determines if it contains any sources as provided by the user. If a processor does not contain any sources, it waits to receive and propagate rays. If it contains sources, it generates a ray for each local source point and target point pair and executes the rays. To make these calls recursive, rays are first generated and then executed once a user defined number of rays has been generated. After a chunk of rays has been executed, a source processor will propagate the generated rays in addition to propagating any other rays that have been received by neighboring processors, and then will again continue generation.

Once ray-tracing is complete, the spatial moments of the uncollided flux are available throughout the domain. This uncollided-flux solution is then used as a first-collision source in Rattlesnake.

4. RESULTS

Thus far, the algorithm described in Section 3.4 has been implemented in Rattlesnake. Also complete is the importation of the cell-averaged uncollided flux as the first-collision source. We present first two simple 3D cases; one with a point source and one with a volumetric source. Last, we present results with problem 3 of the Kobayashi benchmark [10] with and without scattering.

4.1. Point source verification

A point source that emits 1 n/s is located at (0.5, 0.5, 0.5) in a $10 \times 10 \times 2$ mesh of cuboid elements of size [1 cm]^3. The desired quantity is the cell-averaged uncollided flux in each element (the "target" elements) except for the element that contains the source (the element with lower vertex (0, 0, 0) and upper vertex (1, 1, 1)). The total cross section of the medium is then varied and each element evaluated for multiple Gaussian quadratures. The reference solution was evaluated numerically to a relative error tolerance of 1×10^{-12}. The results for two of the target elements are as seen below in Table 1.

4.2. Volumetric source verification

A volumetric source that emits 1 n/cm^3·s is located in the element with corners (0, 0, 0) and (1, 1, 1) in a $10 \times 10 \times 2$ mesh of cuboid elements of size [1 cm]^3 The desired quantity again is

Table 1: Point source to volumetric target results for two elements.

Element (corners)	Quad pts. (1D)	Void		Uniform absorber ($\Sigma_t = 0.5$ cm)	
		Solution	Relative error	Solution	Relative error
(0, 5, 0), (1, 6, 1)	1	3.18309886E-3	3.262E-3	2.61284665E-4	2.146E-2
	2	3.19332170E-3	6.154E-5	2.66929362E-4	3.274E-4
	3	3.19351793E-3	1.007E-7	2.67016540E-4	9.564E-7
	4	3.19351825E-3	6.066E-10	2.67016794E-4	4.799E-9
	5	3.19351825E-3	1.057E-12	2.67016795E-4	1.124E-13
	Ref.	3.19351825E-3		2.67016795E-4	
(0, 5, 1), (1, 6, 2)	1	1.59154943E-3	1.675E-3	4.63828324E-5	1.785E-2
	2	1.59422386E-3	2.087E-6	4.72257415E-5	4.673E-6
	3	1.59422054E-3	8.979E-9	4.72259671E-5	1.036E-7
	4	1.59422053E-3	1.068E-11	4.72259622E-5	5.968E-11
	5	1.59422053E-3	3.128E-15	4.72259622E-5	1.324E-13
	Ref.	1.59422053E-3		4.72259622E-5	

the integrated uncollided flux in each element (the "target" elements) except for the element that contains the source (the element with lower vertex (0, 0, 0) and upper vertex (1, 1, 1)). The total cross section of the targets and source element is varied. The reference solution was obtained by using the ray-tracing implementation with 1000 Gaussian quadrature points per element and four uniform mesh refinements. The results for two of the target elements are as seen in Table 2.

Table 2: Volumetric source to volumetric target results for the element defined by the corners (4, 0, 0) and (5, 1, 1) and the element defined by the corners (8, 0, 0) and (9, 1, 1).

Medium	Quad pts. (1D)	$x = 4$ element		$x = 8$ element	
		Solution	Relative error	Solution	Relative error
Void	1	4.97359197E-3	1.018E-2	1.24339799E-3	2.589E-3
	2	5.02322272E-3	3.044E-4	1.24660216E-3	1.901E-5
	3	5.02474875E-3	7.703E-7	1.24662585E-3	1.322E-8
	4	5.02475259E-3	7.437E-9	1.24662587E-3	2.956E-11
	5	5.02475262E-3	1.990E-11	1.24662587E-3	9.149E-14
	Ref.	5.02475262E-3		1.24662587E-3	
Source $\Sigma_t^s = 0.1$ cm Target $\Sigma_t^t = 0.1$ cm	1	3.33389839E-3	1.505E-2	5.58694732E-4	5.484E-3
	2	3.38349022E-3	4.082E-4	5.61756920E-4	3.394E-5
	3	3.38486842E-3	1.123E-6	5.61775976E-4	2.770E-8
	4	3.38487218E-3	1.046E-8	5.61775991E-4	5.862E-11
	5	3.38487222E-3	2.921E-11	5.61775991E-4	1.377E-13
	Ref.	3.38487222E-3		5.61775991E-4	
Source $\Sigma_t^s = 0.1$ cm Target $\Sigma_t^t = 0.2$ cm	1	2.34935849E-3	1.667E-2	2.63908704E-4	6.833E-3
	2	2.38803761E-3	4.827E-4	2.65711724E-4	4.775E-5
	3	2.38918798E-3	1.291E-6	2.65724404E-4	3.956E-8
	4	2.38919104E-3	1.255E-8	2.65724414E-4	8.844E-11
	5	2.38919107E-3	3.309E-11	2.65724414E-4	1.509E-13
	Ref.	2.38919107E-3		2.65724414E-4	

As the distance between source and target element is increased, the solid angle of the target element as viewed by the source decreases. The solution error then decreases as the source and target distance increases.

4.3. Kobayashi Benchmark

The Kobayashi 3-D benchmark void problems proposed by Kobayashi [10] consist of two sets of one-group source problems with similar geometry. The first set of problems contains void and a pure absorbing medium, while the other replaces the pure absorber with a material which has a scattering cross-section of 50% of the total-cross section. The geometry follows in Figure 2. The total cross sections for regions 1, 2, and 3 are 0.1 cm^{-1}, 10^{-4} cm, and 0.1 cm^{-1}, respectively. The source strength is 1.0 n/cm^3·s. We compare solutions at the 22 points specified in the benchmark.

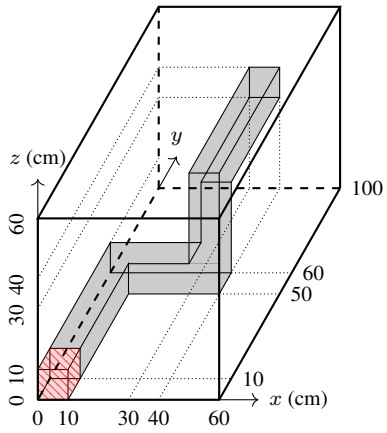

Figure 2: Kobayshi benchmark problem 3 geometry. The red hatched region is region 1 (source), the filled region is region 2 (near void), and the non-filled region is region 3.

As the ray-tracing implementation does not currently support reflecting boundary conditions, one set of the source elements was mirrored across each reflective boundary in the input file. First, the results for Kobayashi problem 3 without scattering are presented. The volumetric source quadrature order is increased to show convergence and an element size of [10 cm]^3 is chosen. Figure 3 shows the errors in the point-uncollided flxues for the problem without scattering, in which higher fidelity reference solutions were obtained from the code developed by Sanchez [11]. General agreement is seen for all points.

For the results with scattering, rays are traced from source elements that contained 343 Gaussian quadrature points each, to target element centroids. Due to the restriction of only cell-averaged values of the uncollided flux, a once-more refined mesh (element sizes of [2.5 cm]^3) was utilized to obtain the uncollided flux. Level-Symmetric quadrature was chosen for the S_N calculation. Figure 4 shows the errors for the case with scattering, with and without uncollided-flux treatment. Significant improvement is seen with the uncollided flux treatment for both the lower and higher order angular quadrature for all but a few of the points in the benchmark.

5. CONCLUSIONS

The uncollided-flux technique has been implemented for arbitrary finite-element meshes in the Rattlesnake code system of the INL. The implementation thus far has been verified and has shown significant improvement in resolving ray effects and shows great potential in application to the

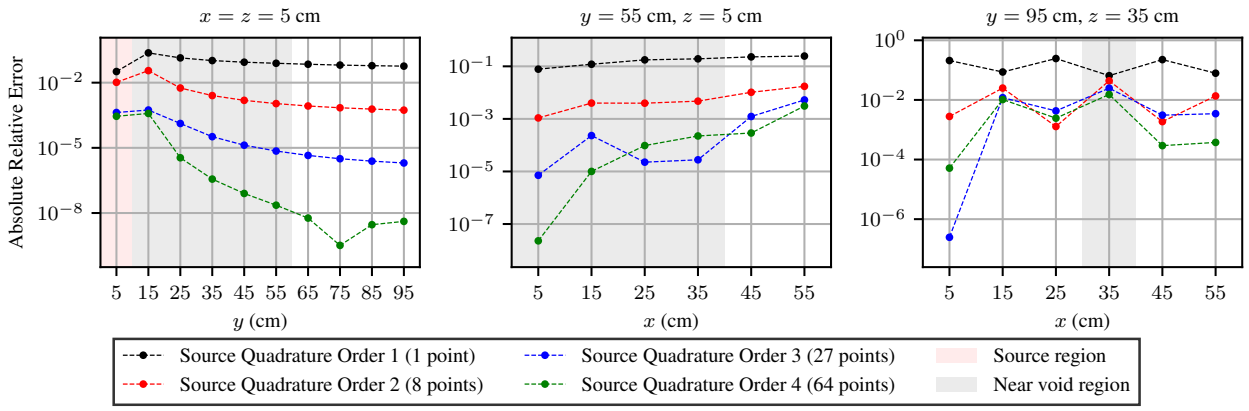

Figure 3: Errors in the point uncollided fluxes for Kobayashi problem 3 without scattering.

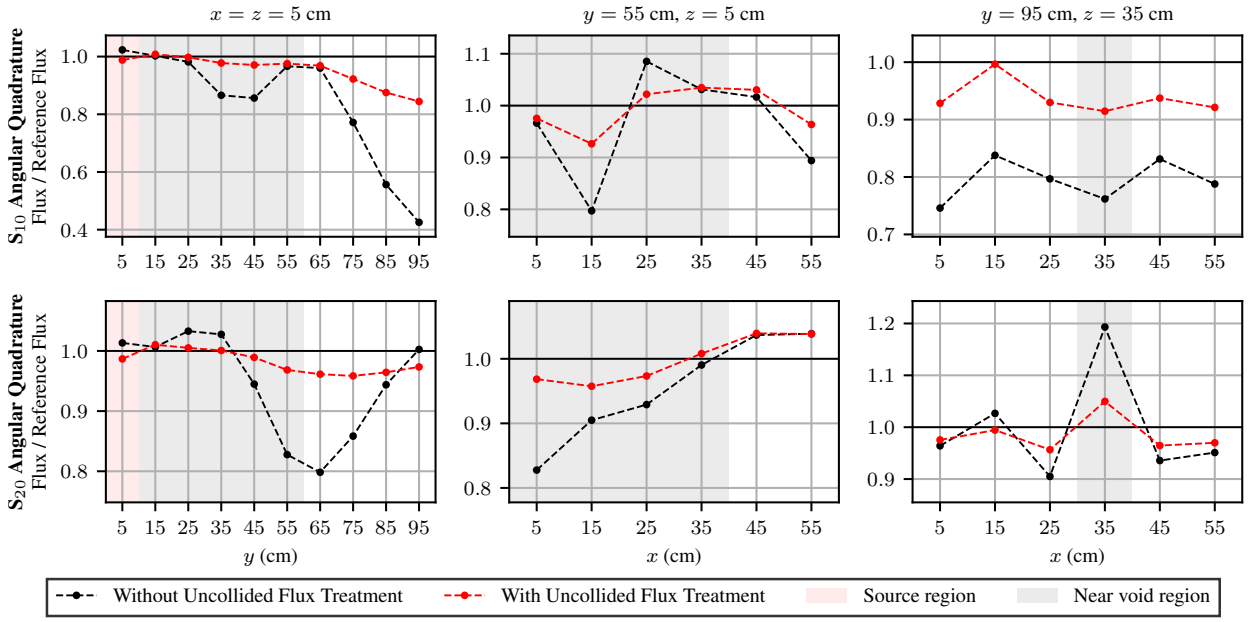

Figure 4: Errors in the point uncollided fluxes for Kobayashi problem 3 with S_{10} and S_{20}.

modeling of systems such as the TREAT hodoscope. Parallel performance studies are currently lacking due to the need to ray-trace on highly-refined meshes, but enabling higher-order uncollided flux solutions will be ground for fair comparisons in the future. Compared to other methods, our treatment presents the following improvements:

- Allows arbitrary sources shapes (most methods allow only point sources);
- Embedded in FEM (finite element method), enabling higher fidelity solutions;
- Easily coupled with other physics as a result of Rattlesnake and the MOOSE framework

ACKNOWLEDGEMENTS

This work is supported by the U.S. Department of Energy, under DOE Idaho Operations Office Contract DE-AC07-05ID14517. Accordingly, the U.S. Government retains a nonexclusive, royalty free license to publish or reproduce the published form of this contribution, or allow others to do so, for U.S. Government purposes.

REFERENCES

[1] K. D. Lathrop. "Ray effects in discrete ordinates equations." *Nuclear Science and Engineering*, **volume 32**(3), pp. 357–369 (1968).

[2] D. Chichester, S. Watson, J. Johnson, and D. Wachs. "The TREAT Fast-Neutron Hodoscope and Plans for Restoring it to Operation." *Transactions of the American Nuclear Society*, **volume 113**, pp. 377–380 (2015).

[3] T. Wareing, J. Morel, and D. Parsons. "A first collision source method for ATTILA, an unstructured tetrahedral mesh discrete ordinates code." Technical report, Los Alamos National Lab., NM (United States) (1998).

[4] J. W. Kim and Y.-O. Lee. "AETIUS solutions for Kobayashi 3D benchmarks with the first collision source method on the volume source and unstructured tetrahedral mesh." *Annals of Nuclear Energy*, **volume 113**, pp. 446 – 469 (2018). URL http://www.sciencedirect.com/science/article/pii/S0306454917304255.

[5] R. E. Alcouffe. "Partisn calculations of 3D radiation transport benchmarks for simple geometries with void regions." *Progress in Nuclear Energy*, **volume 39**(2), pp. 181 – 190 (2001). URL http://www.sciencedirect.com/science/article/pii/S0149197001000117.

[6] T. M. Evans, A. S. Stafford, R. N. Slaybaugh, and K. T. Clarno. "Denovo: A new three-dimensional parallel discrete ordinates code in SCALE." *Nuclear technology*, **volume 171**(2), pp. 171–200 (2010).

[7] R. Lillie. "GRTUNCL3D: A discontinuous mesh three-dimensional first collision source code." In *Proc. ANS Topl. Mtg. Radiation Protection and Shielding*, volume 1, p. 368. American Nuclear Society LaGrange Park, IL (1998).

[8] K. Kosako and C. Konno. "FNSUNCL3: first collision source code for TORT." *Journal of Nuclear Science and Technology*, **volume 37**(sup1), pp. 475–478 (2000).

[9] D. Gaston, B. Forget, K. Smith, and R. Martineau. "Verification of MOCkingbird, Unstructured-Mesh, Method of Characteristics Implementation Using the MOOSE Multiphysics Framework." In *International Conference on Mathematics and Computational Methods Applied to Nuclear Science and Engineering, M&C 2017* (2017).

[10] K. Kobayashi. "A proposal for 3-D radiation transport benchmarks for simple geometries with void region." In *3-D deterministic radiation transport computer programs. Features, applications and perspectives* (1997).

[11] I. Suslov, R. Sanchez, and I. Zmijarevic. "Deterministic Reference Solution for 3-D Kobayashi Benchmarks." *M&C*, **volume 99**, p. 1765 (1999).